Characteristics of Photodissociation at 193 nm of Singly Protonated Peptides Generated by Matrix-Assisted Laser Desorption Ionization (MALDI)

Kyung Mi Choi, So Hee Yoon, Meiling Sun, Joo Yeon Oh,*
Jeong Hee Moon,† and Myung Soo Kim

National Creative Research Initiative Center for Control of Reaction Dynamics and School of Chemistry, Seoul National University, Seoul, Korea

Photodissociation (PD) at 193 nm of various singly protonated peptides was investigated. These include peptides with an arginine residue at the *C*-terminus, *N*-terminus, at both termini, inside the chain, and those without an arginine residue. Monoisotopomeric selection was made for the precursor ions. Interference from the post-source decay (PSD) product signals was reduced as much as possible by using the deflection system (reported previously) and subtracting the remaining signals from the laser-on signals. The presence of an arginine residue and its position inside the peptide were found to significantly affect the PD spectra, as reported previously. Presence of a proline, aspartic acid, or glutamic acid residue hardly affected the PD spectral patterns. By comparing the PD spectra obtained at a few different wavelengths, it is concluded that the dissociation of the photoexcited ions occurs in their ground electronic states. Tentative explanations for the observed spectral correlations based on the statistical picture for the reactions are also presented. (J Am Soc Mass Spectrom 2006, 17, 1643–1653) © 2006 American Society for Mass Spectrometry

Tandem mass spectrometry (MS/MS) [1] is a useful technique to study the structure and fragmentation mechanism of gas-phase ions. With the development of various techniques to generate gas-phase ions from condensed-phase samples such as electrospray ionization (ESI) [2] and matrix-assisted laser desorption ionization (MALDI) [3], MS/MS has been widely used to study biological molecules, and most importantly, peptides and proteins.

Ions formed with sufficient internal energy in the source may dissociate after exiting the source. This is called the metastable ion decomposition [4]. Post-source decay (PSD) [5] is the terminology for a similar phenomenon observed in tandem time-of-flight (TOF) mass spectrometry for ions that are generated by MALDI. Ions may be further activated to expedite their dissociation. Collisionally activated dissociation (CAD) [6, 7], infrared multiphoton dissociation (IRMPD) [8], surface-induced dissociation (SID) [9, 10], and electron capture dissociation (ECD) [11, 12] are widely used for this purpose.

PSD, low-energy CAD and SID, and IRMPD of peptide ions have been popular in the bottom-up strategy [13] for protein identification and de novo sequencing [14]. In these schemes, both ion activation and dissociation occur in the ground electronic state of the precursor ion. It is well known that the critical energy is one of the two most important parameters (the other is the entropy of activation) that affect the rate of a statistical reaction [15, 16]. Dissociation of peptide ions using the above MS/MS schemes usually results in y- and b-type product ions, which are the ions formed via reaction paths with small critical energy, and a-type ions with lesser intensity and frequency. It is also known that b-type ions are prominent with an arginine residue at the *N*-terminus of the peptide while y-type ions are prominent with the same residue at the *C*-terminus [17]. Some residue-specific dissociations have also been noticed, and they may be utilized for spectral interpretation. These include the preferential cleavages at the *N*-terminal side of the proline residue [18, 19] and at the *C*-terminal side of the aspartic acid, glutamic acid, and histidine residues [20]. It is known that "the mobile proton model" [20] provides an adequate explanation for some of these spectral correlations, which may be regarded as a mechanistic version of the energetics argument mentioned above.

Photodissociation (PD) in the ultraviolet range, UV-PD, is a useful technique to study the structure, kinetics

Published online August 24, 2006

Address reprint requests to Dr. M. S. Kim, School of Chemistry, Seoul National University, Seoul 151-742, Korea. E-mail: myungsoo@snu.ac.kr

* Current address: Laboratory for Organic Chemistry, Swiss Federal Institute of Technology, ETH Hönggerberg, 8093 Zürich, Switzerland.

† Current address: Korea Research Institute of Bioscience and Biotechnology, Daejeon 305-806, Korea.

1044-0305/06/$32.00
doi:10.1016/j.jasms.2006.07.021

Received May 23, 2006
Revised July 15, 2006
Accepted July 19, 2006

and dynamics of molecular ions [21, 22]. However, its application to biological samples is not common yet, partly because of the poor quality of the photofragment spectra reported thus far, in comparison with PSD and CAD spectra. The situation has been changing in recent years with the development of instrumental methods to improve the spectral quality [23–28]. This laboratory has been designing, constructing, and optimizing tandem TOF mass spectrometers to study the photodissociation of peptide ions generated by MALDI. Monoisotopomeric selection of a precursor ion was achieved by using ion pulse-PD laser pulse synchronization. Product ion resolution has been improved by using a reflectron with linear-plus-quadratic potential inside [23]. In addition, the background noise was greatly suppressed by eliminating as much as possible the chemical and electrical noises [25]. In our initial attempt, product ion spectra were recorded without (laser-off or PSD) and with (laser-on) the PD laser, and the former spectrum was subtracted from the latter spectrum to obtain the laser-induced change or the PD spectrum. However, the method was not quite adequate to eliminate contamination by PSD product ions. The critical problem was that some of the PSD product ions, which moved together with their precursor ion, underwent photodissociation themselves. This often led to a negative signal in the final PD spectrum. Later, a deflection system was installed between the ion source and the ion gate to eliminate as much as possible PSD product ions forming in front of the ion gate [28].

The UV-PD of peptide ions is different from PSD and low-energy CAD in two respects. First, the state accessed by photoexcitation in the UV range is an excited electronic state. Second, the magnitude of the internal energy gained by photoabsorption is relatively large (energy of 193 nm photon is 6.42 eV) and can be even larger with multiphoton absorption. A molecule prepared in an excited electronic state by absorption of a UV photon may undergo dissociation by various processes. Direct dissociation from a repulsive electronic state is the usual mechanism for diatomic and some triatomic molecules. For a large polyatomic cation, it is quite common for the electronically excited molecule to undergo a rapid radiationless transition to the ground electronic state and to dissociate in the latter state. The theory of mass spectra, or the quasiequilibrium theory [29], further postulates that the vibrational or internal energy thus obtained is redistributed rapidly by intramolecular relaxation (IVR) before dissociation. Hence, whether the dissociation occurs in the excited or ground electronic state, and should it occur in the ground state, whether it would occur after statistical distribution of the vibrational energy, are important issues for PD in the UV range.

So far, successful PD of singly protonated peptides has been reported at 266, 193, and 157 nm. Previously [30, 31], we reported 266 nm PD for the peptide ions of the type $[RGGXGGGGGR + H]^+$ with various amino acid residues as X. PD was efficient when X was one of the tryptophan, tyrosine, or phenylalanine residue. It was thought that the $\pi_A^* \leftarrow \pi_A$ transition localized at the aromatic residue (A) was responsible for the absorption at 266 nm. An interesting observation was that cleavages of the peptide bonds at both ends of the chromophore were found to be particularly dominant. In the absence of these residues, over ten times stronger laser intensity was needed, and most of the peptide bonds in the cation cleaved with similar probability. Participation of two dissociation mechanisms, one that occurred before IVR and another that occurred after IVR, was suggested for the PD of the peptide ions with an aromatic residue, which were called nonstatistical and statistical mechanisms, respectively.

Even though PD at 193 nm was attempted much earlier than at any other wavelength [27, 32, 33], there has been little discussion on the photophysics and chemistry involved. It is well known [34] that a peptide bond (P) absorbs efficiently at around 190 nm due to the $\pi_P^* \leftarrow \pi_P$ transition and, hence, the excited state accessed at 193 nm must have the $\pi_P\pi_P^*$ character. Recently, Morgan and Russell [35] studied the effects of charge site and fragmentation time scale in 193 nm PD for cationized bradykinin and some of its analogs. They concluded that the dissociation of the photoexcited peptide ions proceeded via the conventional statistical scheme.

PD at 157 nm for singly protonated peptides was reported by Reilly et al. [26, 36]. The fragmentation patterns at this wavelength were strikingly different from those in the PSD and low-energy CAD spectra. Namely, the 157 nm PD spectra were dominated by the contiguous series of x_n and a_n ions depending on whether the arginine residue was at the *C*- or *N*-terminus. They suggested that an excited electronic state(s) with the $n_P\pi_P^*$ character was accessed by absorption at 157 nm. Furthermore, they suggested that this state was dissociative and that the cleavage of the bond between the α-carbon and the carbonyl carbon occurred via a Norrish Type I process that initially generated $x_n + 1$ and $a_n + 1$ radical cations depending on the position of the arginine residue. Then, generation of even electron ions such as x_n, w_n, v_n, a_n, and d_n were attributed to consecutive losses of radical neutrals from the radical cations. The beauty of the whole scheme was that it readily explained the striking spectral variation due to the arginine position. However, it was recently observed [37] that PD spectra for singly protonated peptides at 193 nm displayed similar characteristics to those at 157 nm, thereby raising some doubts on the interpretation of the latter spectra by Reilly et al.

This paper provides an overview on the general characteristics of PD at 193 nm of singly protonated peptides that was garnered by experiments on numerous samples, and presents some possible explanations.

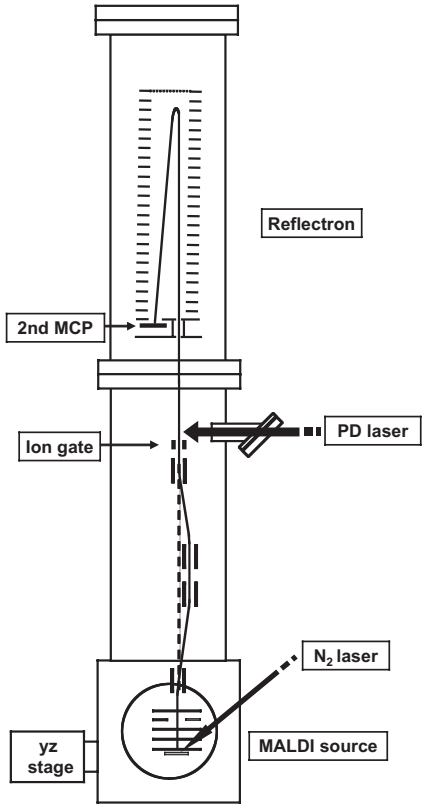

Figure 1. A schematic of the homebuilt MALDI-tandem TOF mass spectrometer equipped with a deflection system used in the present PD study.

Experimental

Figure 1 shows a schematic of the homebuilt MALDI-tandem TOF mass spectrometer equipped with a deflection system used in this PD study. Details of the original instrument, the deflection system, and the operational method were described in previous reports [23–25, 28]. A brief outline follows.

The instrument consists of a MALDI source with delayed extraction, a first stage TOF analyzer to time-separate the prompt ions generated in the source, an ion gate, and a second stage TOF analyzer that utilizes a reflectron with linear-plus-quadratic potential inside. A deflection system consisting of four bipolar deflectors is installed between the ion source and the ion gate. The low-resolution ion gate (around 30 resolving power) selects a precursor ion while the deflection system eliminates most of the PSD product ions formed before the final deflector. Typical DC voltages applied to the sample plate and the final electrode of the reflectron are 20 and 25 kV, respectively, while ±1 kV is applied to each bipolar deflector. MALDI is achieved by a N_2 laser (MNL205-C, Lasertechnik, Berlin, Germany). At some time after the MALDI laser irradiation, a pulse of 1.8 kV is applied to the sample plate for delayed extraction. To record a PD laser-on spectrum, a cylindrically focused laser beam at 193 nm (PSX-100, MPB Communications, Montreal, Quebec, Canada) or at 266 nm (Surelite III-10, Continuum, Santa Clara, CA) is irradiated at the first time focus, which is located immediately after the ion gate. The PD laser pulse is synchronized with the A peak (the lowest-mass isotopomer) of the precursor ion for the isotopomer selected photodissociation. The PSD spectrum under the same experimental condition is recorded without the PD laser. The output from the MCP detector is sent to an A/D card (CS82G, Gage Applied Technologies, Montreal, Quebec, Canada) and digitized. Before spectral averaging, the electrical noise in each MALDI shot is eliminated as much as possible by following the method described previously [25]. Each averaged spectrum is reduced into a bar graph. Finally, the PSD spectrum is subtracted from the laser-on spectrum to obtain the PD laser-induced change or the PD spectrum.

The peptide samples RGGYGGGGGR and RLLAPITAY with 98% purity were purchased from Peptron (Daejeon, Korea). The peptide samples EGVNDNEEGFFSAR, MEHGRWG, RPPGFSPF, RPPGFSPFR, YPFVEPI, and YPYDVPDYA and the matrix [α-cyano-4-hydroxycinnamic acid (CHCA)] were purchased from Sigma (St. Louis, MO). A matrix solution was prepared daily using acetonitrile and 0.1% trifluoroacetic acid that was mixed with a peptide solution. The final peptide concentrations prepared for PD experiments were 10 pmol/μl. One μl of the solution was loaded on the sample plate.

Results

The use of the deflection system is important for the PD study of the peptide ions $[YPFVEPI + H]^+$ and $[YPYDVPDYA + H]^+$ investigated in this work because these model systems, without an arginine residue, show very strong PSD signals. In the PSD spectra for $[YPFVEPI + H]^+$, Figure 2a, several strong peaks appear, which are primarily b-, a-, and y-type ions. The intensities of these peaks decrease substantially as deflector potentials are turned on, as can be seen from the deflector-on spectrum shown in the same figure. Taking the intensities of the b_4 and b_5 peaks as references, PSD signals in the deflector-on spectrum are about 23% of those in the deflector-off spectrum. According to our estimate, most of the remaining intensities are attributable to PSD occurring after the deflection system, substantial fractions of which occur after the first time focus or the PD laser irradiation spot. Intensities of some peaks such as a_4, a_5, PFV, and PFVE decrease more than those of b- and y-type peaks. This was explained in our previous report by assuming that the former ions were formed via consecutive reactions. Figure 2b shows the 193 nm PD spectra obtained with the deflector voltages off and on. Note that the deflector-off spectrum shows strong negative signals for ions such as a_4, a_5, b_4, b_5, y_6, and PFVE that appear prominently in the PSD spectrum because of the photodissociation of the PSD product ions themselves. The number of negative signals in the deflector-on PD spectrum is less and their intensities are

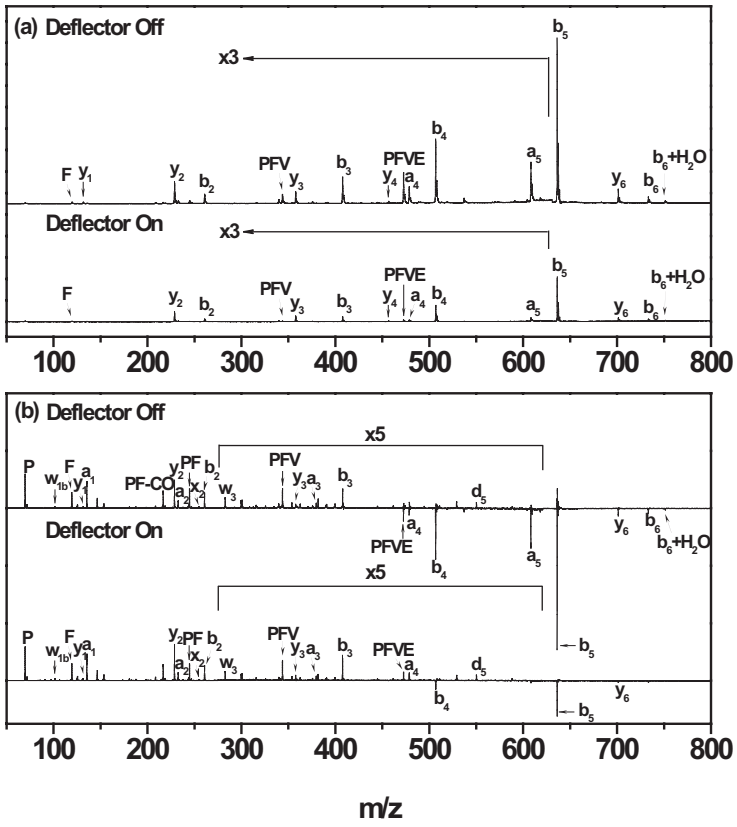

Figure 2. (**a**) PSD and (**b**) 193 nm PD spectra for $[YPFVEPI + H]^+$ obtained with deflector voltages off and on.

weaker than in the deflector-off spectrum. More importantly, some ions such as a_4, which are difficult to recognize in the deflector-off spectrum, are clearly seen in the deflector-on spectrum. Since the sign and magnitude of a signal in a PD spectrum would be principally determined by the competition between PD of the PSD product ion and the photogeneration of the same ion from the precursor, the above observation means that the deflection system has successfully eliminated substantial fractions of the PSD product ions formed in front of the PD laser irradiation spot. The situation is similar for $[YPYDVPDYA + H]^+$ whose PSD and 193 nm PD spectra are shown in Figure 3, namely, b_5, b_7, b_8, and y_8, which are prominent in the PSD spectrum, appear as negative signals in the PD spectrum. PD spectra such as in Figures 2b and 3b have been further processed using the spectral reduction method reported previously [25]. Negative signals have been eliminated from the reduced spectra, which will be presented hereafter. Table 1 provides a brief summary of major product ion types generated by PSD and PD.

Arginine Effect

Previously, we reported our preliminary results from 193 nm PD study for singly protonated peptides [37]. The main purpose of the work was to demonstrate that excellent quality PD spectra could be obtained at 193 nm and that the spectral patterns at 193 nm were quite similar to those at 157 nm reported by Reilly et al. [26, 36]. As with PD at 157 nm, the 193 nm PD spectra for singly protonated peptides with an arginine residue at the *C*-terminus were dominated by the x-, v- and w-type product ions, while a- and d-type ions dominated when the same residue was at the *N*-terminus. In particular, the peptide ions investigated displayed a complete series of x_n and a_n product ions, depending on the position of the arginine residue, which also agreed with Reilly's results at 157 nm. After the above preliminary work, we recorded 193 nm PD spectra for many other singly protonated peptides with an arginine residue at the *C*- or *N*-terminus. In all the cases studied, the same spectral correlation as above was observed. Figure 4a provides an example for the peptides with an arginine residue at the *N*-terminus, the 193 nm PD spectrum for $[RPPGFSPF + H]^+$. It is seen that a complete series of a_n appear in this spectrum. The 193 nm PD spectrum for $[EGVNDNEEGFFSAR + H]^+$ was shown in the previous report [37]. However, Figure 4b replicates it for reasons to be explained later. The latter PD spectrum is dominated by the *C*-terminal fragments, x_n, y_n, v_n, and w_n.

Figure 5 shows the 193 nm PD spectrum for $[MEHFRWG + H]^+$, which has an arginine residue inside the chain and, according to the above correlation, is expected to generate prominent a_5, a_6, and x_3-x_6 ions. Even

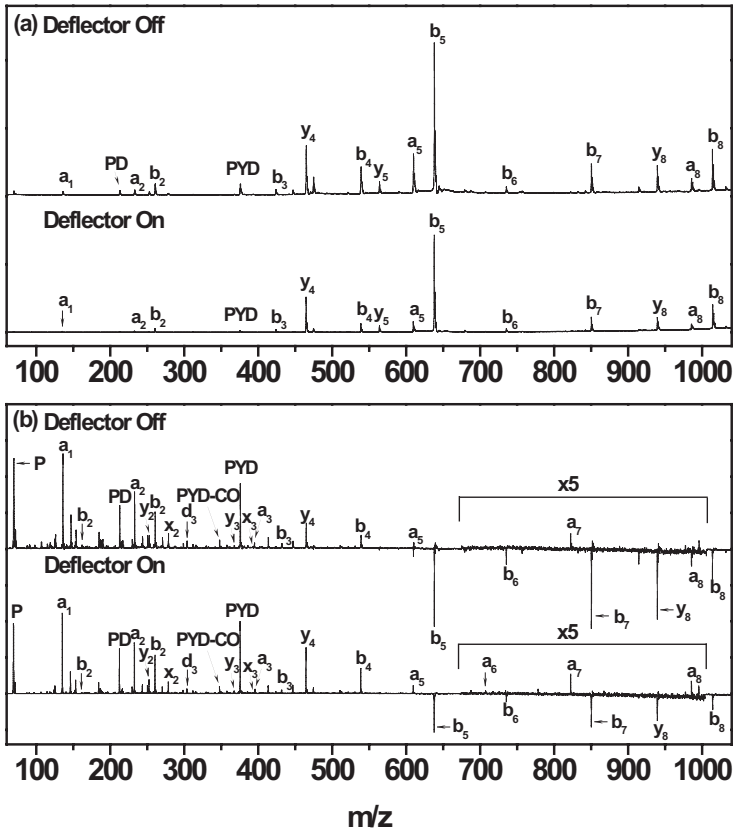

Figure 3. (**a**) PSD and (**b**) 193 nm PD spectra for $[YPYDVPDYA + H]^+$ obtained with deflector voltages off and on.

though a complete series of a_n ions appear in the spectrum, the a_5 and a_6 are stronger than the others in the series. This agrees with our expectation. Similarly, x_3–x_6 ions are stronger than x_1 and x_2; x_2 is barely observed in the spectrum. A similar trend was seen in 193 nm PD of protonated angiotensin II reported previously [37]. The trend observed thus far can be summarized as the spectral correlation that a_n appears prominently when an arginine residue is present at some position toward the *N*-terminal side of the peptide bond cleaved while x_n appears with the same residue toward the *C*-terminal side.

We also studied 193 nm PD of some peptides with arginine residues at both termini. Figure 6 shows two typical results: PD spectra for $[RGGYGGGGGR + H]^+$ and $[RPPGFSPFR$ (bradykinin) $+ H]^+$. A high quality PD spectrum for the latter peptide ion was rather difficult to record with the previous instrument without the deflection system because of the presence of very strong PSD signals. Note also that a_4 and v_7 are the most prominent peaks in the high *m/z* region of the 193 nm PD spectrum for $[RGGYGGGGGR + H]^+$. These are the peaks attributable to the cleavages occurring at the *C*- and *N*-terminal sides of the tyrosine (Y) residue. Prominence of these peaks was also seen in the 266 nm PD spectrum. More importantly, a complete series of x_n (x_1–x_8) and a_n (a_1–a_9) appear in the 193 nm PD spectrum. This is in accord with the spectral correlation mentioned above. It is interesting to note that a_n+1 peaks also appear, sometimes prominently. In the case of protonated bradykinin (Figure 6b), a complete series of a_n (a_1–a_8) prominently appear, but x_n ions are not as prominent with the exception of x_5 and x_6.

Finally, we studied 193 nm PD of singly protonated peptides with no arginine residue. $[YPFVEPI + H]^+$ and $[YPYDVPDYA + H]^+$, whose PSD and PD spectra were shown in Figures 2 and 3, are such examples. The PD spectrum for $[YPFVEPI + H]^+$ is characterized by

Table 1. Major fragment ion types generated by PSD and PD of protonated peptides

Peptide feature	PSD fragments	266 nm PD fragments	193 nm PD fragments
Arginine at *C*-terminus	b, y	b, x, y, w	x, v, w
Arginine at *N*-terminus	a, b, y	a, b, d	a, d
Arginine at both termini	b, y	a, x, y, z	a, x, y, z
Arginine inside the chain	a, b, y	—	a, x, y
Without an arginine	a, b, y	—	a, b, y

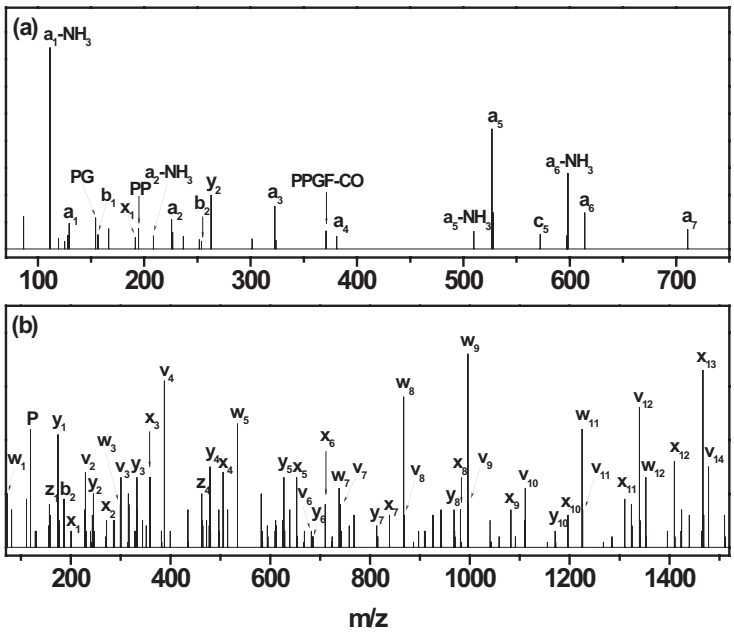

Figure 4. The 193 nm PD spectra for (**a**) $[RPPGFSPF + H]^+$ and (**b**) $[EGVNDNEEGFFSAR + H]^+$ after spectral reduction.

the presence of a_n (a_1–a_4), b_n (b_2 and b_3), y_n (y_1–y_3), and several internal fragment ions such as PF and PFV, which mostly occur in the lower *m/z* half of the spectrum. On the other hand, x_2, w_3, and d_5 weakly appear, which are the ions characteristic of 193 nm PD. From the appearance of a_1–a_4 and d_5, one may presume that the spectrum resembles the ones obtained for the peptide ions with an arginine at the *N*-terminus and that the basicity of the amine group at the *N*-terminus is responsible for the resemblance. However, remember that the negative peaks at the higher *m/z* half of the PD spectrum appear for the fragment ions with strong PSD intensity, that the PSD intensities in this case are much stronger than for those with an arginine residue, and that a PD intensity is determined by competition between PD of PSD and photogeneration from the precursor ion. In that case, PD of the precursor ion might have generated a_5, b_4, b_5, b_6, and y_6 ions even though these ions show negative peaks in the PD spectrum. That is, the fragment ions generated by 193 nm PD of $[YPFVEPI + H]^+$ may be similar to those generated by PSD, and the differences between the two spectra are primarily due to the difference in the precursor ion internal energy. In the PD spectrum for $[YPYDVPDYA + H]^+$ Figure 3b, negative signals appear for b_5, b_7, b_8, and y_8, which are strong peaks in the PSD spectrum. Since y_4 is another strong peak in the PSD spectrum, one expects a negative signal at this position. However, y_4 is a strong

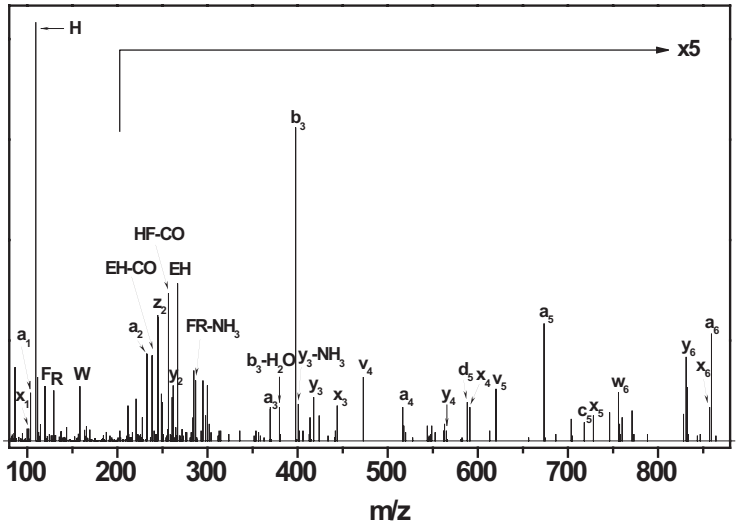

Figure 5. The 193 nm PD spectrum for $[MEHFRWG + H]^+$ after spectral reduction.

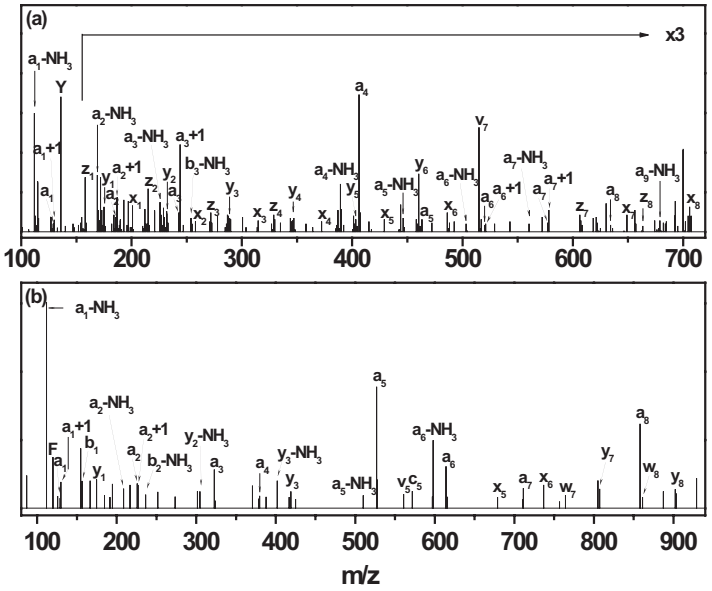

Figure 6. The 193 nm PD spectra for (**a**) $[RGGYGGGGGR + H]^+$ and (**b**) $[RPPGFSPFR + H]^+$ after spectral reduction.

positive peak, which suggests that it must have been abundantly formed by 193 nm PD. Other features in the PD spectrum are similar to the previous case of $[YPFVEPI + H]^+$; a_n (a_1–a_8), b_n (b_1–b_4), y_n (y_1–y_5), and internal fragment ions such as PYD appear in the PD spectrum. In particular, more a_n and internal fragment ions appear in the 193 nm PD spectrum than in the PSD spectrum; x_1, x_2, x_3, and d_3 are minor features of the spectrum. To summarize, the x_n and a_n ions, which are the characteristic ions in 193 and 157 nm PD of the peptide ions with an arginine residue, are far less conspicuous in its absence.

Residue-Specific Dissociation

As mentioned above, the *N*-terminal side of a proline residue, the *C*-terminal sides of aspartic and glutamic acid residues in the absence of a mobile proton, and the *C*-terminal side of a histidine residue in the presence of a mobile proton tend to cleave preferentially in the low-energy regime. Since these effects do not universally occur even in the low-energy regime, studies on a statistically meaningful number of samples are needed to establish whether the same effects also occur in 193 nm PD. Despite this, results from the studies on a limited number of samples are presented just to gain some qualitative insight.

Let us first consider the proline effect for the peptide ions without an arginine residue studied above: $[YPFVEPI + H]^+$ and $[YPYDVPDYA + H]^+$. In the PSD spectrum for $[YPFVEPI + H]^+$ (Figure 2a), b_5 is the strongest peak in agreement with the correlation reported by Wysocki et al. [19] that the E—P bond is easily cleaved. As mentioned above, whether the same ion would be abundantly formed in 193 nm PD cannot be definitively determined because the b_5 ion itself undergoes a strong photodissociation at this wavelength. On the other hand, the y_2 peak, which is not particularly strong in the PSD spectrum, is the strongest peak in the PD spectrum (Figure 2b). This might not be evidence for the proline effect because other low *m/z* ions also prominently appear in the PD spectrum, such as a_1 and b_2. In particular, the latter ion, which is formed via cleavage of the peptide bond between P and F, is relatively stronger than in the PSD spectrum. Note that the cleavage at the *C*-terminal side of the proline is unfavorable in the low-energy regime. The situation is similar for $[YPYDVPDYA + H]^+$. Namely, even though it is uncertain whether b_5 is abundantly formed, y_4 is a strong peak in the PD spectrum (Figure 3b), which agrees with the correlation that the V—P bond is labile. However, a_2 and b_2 also prominently appear in the PD spectrum, which disagrees with the correlation observed in the low-energy regime. The proline effect in 193 nm PD can barely be noticed in the case of $[RLLAPITAY + H]^+$. Here, y_5, b_4, and b_4-NH_3 are strong peaks in the PSD spectrum (not shown), which agrees with the correlation that the A—P bond is rather labile. On the other hand, a_4 is one of the weakest of the a_n ions in the 193 nm PD spectrum as previously reported [37]. In the PSD spectrum (not shown) of $[RPPGFSPF + H]^+$ dealt with above, b_6 and y_7 prominently appear in spite of the correlation that the S—P and R—P bonds are not quite labile. On the other hand, a_6 is not particularly strong in the 193 nm PD spectrum (Figure 4a). Similarly, even though the PSD spectrum (not shown) for $[RPPGFSPFR + H]^+$ indicates that the S—P bond is labile, a_6 is not particularly strong while x_3 is barely observed in the 193 nm PD spectrum (Figure 6b). Overall, it seems that the proline effect is not important in 193 nm PD,

especially when an arginine residue is present, even though it might operate somewhat when arginine is absent.

Since we are dealing with singly protonated peptides, the acid effect is operative only when arginine is present. Let us first consider the acid effect in [EGVNDNEEGFFSAR + H]$^+$, which was dealt with above. Its PSD spectrum (not shown) is dominated by y_6, y_9, and y_{13} due to the presence of glutamic (E) and aspartic (D) acids. In particular, y_9 is stronger than y_6 and y_{13} by a factor of two. Even though w_9 and x_{13} are stronger than others in its PD spectrum (Figure 4b), their dominance is not as spectacular as in the PSD spectrum. In addition, x_6 is only a medium intensity peak in the spectrum. In the [MEHFRWG + H]$^+$ dealt with above, y_5 is the dominant peak in the PSD spectrum (not shown) in agreement with the glutamic acid effect. On the other hand, x_5 is only a weak feature in its PD spectrum (Figure 5). In the 193 nm PD spectrum of the protonated angiotensin II (DRVYIHPF) reported previously [37], x_7 was a minor feature, while y_7 dominated in the PSD spectrum because of the presence of aspartic acid. Similarly, even though y_3 was the dominant peak in the PSD spectrum for [FSWGAEGQR + H]$^+$ because of the presence of glutamic acid, x_3 was one of the weak peaks among x_n ions in the 193 nm PD spectrum as reported previously [37]. The evidence presented so far suggests that the acid effect is not operative in 193 nm PD.

For the singly protonated peptides studied in this work, the histidine effect can be operative when arginine is absent. The histidine effect in 193 nm PD could not be tested because good PD spectra for such samples could not be recorded. However, we are pessimistic about the effectiveness of the histidine effect in consideration of the results of the acid effect.

Discussion

As mentioned above, high quality 193 nm PD spectra for singly protonated peptides obtained in this laboratory [37] were very similar to the corresponding 157 nm spectra reported by Reilly et al. In particular, all the (x_n, v_n, w_n) or (a_n, d_n) ions observed in the 157 nm spectra also appeared in the 193 nm spectra. One can devise a few possible scenarios to explain such a spectral similarity. The first is to accept Reilly's scenario for 157 nm PD and to suppose that a similar scheme also applies to 193 nm PD. It would be a coincidence, however, if the two independent states, $n_P\pi^*_P$ and $\pi_P\pi^*_P$, resulted in the same repulsive reaction. The second scenario is to assume that the $n_P\pi^*_P$ state undergoes internal conversion to the $\pi_P\pi^*_P$ state and that the latter is a dissociative state. A third scenario is to accept the conventional theory of mass spectra, as did Morgan and Russell [35]; namely, to postulate rapid conversion from both states to the ground electronic state and dissociation thereafter.

Two features in our 193 nm PD spectra, which were not noted in the earlier report, should be mentioned in this regard. Before presenting these, we emphasize that the PSD contribution has been eliminated as far as possible in the PD spectra obtained in this laboratory, and that the fragment ions appearing in the PD spectra are isotopically pure because an isotopomeric selection has been made for the precursor ions. The first feature is that even though the x_n ions appeared contiguously in the 193 nm PD spectra for peptide ions with an arginine residue at the *C*-terminus, peaks at the x_n+1 positions were very rare. For the peptide ions with an arginine residue at the *N*-terminus, peaks were observed occasionally at the a_n+1 positions. Even when a peak appeared at the a_n+1 position, however, it was usually weaker than the a_n peak. Even though this phenomenon might be explained by assuming very rapid loss of a hydrogen atom from x_n+1 or a_n+1, it is rather awkward to accept a Norrish Type I cleavage occurring from a dissociative electronic state when most of the x_n+1 ions and many of the a_n+1 ions are missing. In the 193 nm PD spectrum for [RGGYGGGGGR + H]$^+$ obtained in this work, some a_n+1 peaks appear prominently, which might be considered as a partial support for the repulsive mechanism. However, the peaks at the x_n+1 position are also very rarely observed in this case. Thus, it is again awkward to postulate that repulsive dissociation occurs when the attached proton is at the *N*-terminus arginine residue but it does not when the proton is at the *C*-terminus residue.

The second feature is that some b_n and y_n ions also appeared in the 193 nm PD spectra. These ions would not be generated from an excited-state that is repulsive with respect to the bond between the α-carbon and the carbonyl carbon. Some of these ions also appeared in the 157 nm PD spectra even though they have a somewhat lesser frequency and intensity than in 193 nm PD. Reilly et al. [36] suggested that they might be contributions from PSD. The same explanation does not apply to the 193 nm PD spectra obtained in this laboratory because the PSD contributions were almost completely eliminated.

The fact that b_n and y_n, which are the main product ions generated in the low-energy regime, are also observed in 157 and 193 nm PD and that their intensity and frequency of appearance increases as the photon energy decreases would suggest the possibility that all the dissociations competitively occur in the ground electronic state. That is to say, the observations made thus far are compatible with the conventional theory of mass spectra as far as generation of x_n and a_n are energetically more unfavorable but entropically more favorable than that of b_n and y_n, in agreement with Morgan and Russell. To test the possibility, we recorded 266 nm PD spectra for some peptide ions that were investigated at 157 and/or 193 nm. Figure 7 shows three typical results for [EGVNDNEEGFFSAR + H]$^+$, [RGGYGGGGGR + H]$^+$ and [RLLAPITAY + H]$^+$. In the 266 nm PD spectrum of the first ion (Figure 7a), b_n, y_n, and w_n peaks prominently appear. Many x_n peaks can

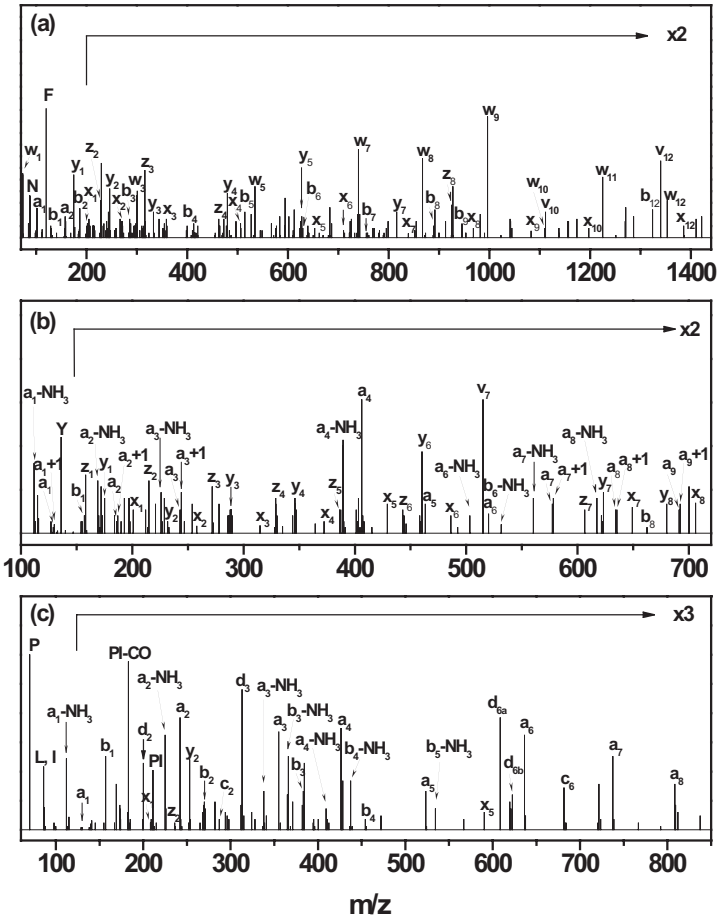

Figure 7. The 266 nm PD spectra for (**a**) $[EGVNDNEEGFFSAR + H]^+$, (**b**) $[RGGYGGGGGR + H]^+$, and (**c**) $[RLLAPITAY + H]^+$ after spectral reduction.

be identified, x_1–x_{10} and x_{12}, even though with much weaker intensities than in the 193 nm PD spectrum shown in Figure 4b. In the spectrum for the second ion (Figure 7b), a weak but contiguous series of x_n ($n = 1$–8) ions can be seen even though a_n and y_n ions dominate the spectrum. Particularly interesting is that some $a_n + 1$ peaks such as $a_7 + 1$, $a_8 + 1$, and $a_9 + 1$ prominently appear in this spectrum. Finally, the 266 nm PD spectrum for the third ion (Figure 7c) is dominated by the contiguous series of a_n (a_1–a_8) and some d_n (d_2, d_3, and d_6). Since aromatic residues, F or Y, are present in the above precursor ions, the excitation at 266 nm is expected to initially generate localized $\pi_A\pi_A^*$ states at these residues. Even though the high-energy product ions such as x_n and a_n distinctly appear in their 266 nm PD spectra, it is improbable that the $\pi_A\pi_A^*$ states are other dissociative electronic states that lead to Norrish Type I processes. Also, the prominent appearance of some $a_n + 1$ peaks in 266 nm PD of $[RGGYGGGGGR + H]^+$ suggests that the presence of these ions cannot be evidence for the repulsive cleavage of the bond between the α-carbon and carbonyl carbon. Probably, these ions can be generated by a mechanism other than the repulsive one.

It is interesting to note that a_n, b_n, and y_n ions dominate the 193 nm PD spectra in Figures 2b and 3b, respectively, for the peptide ions without an arginine residue, $[YPFVEPI + H]^+$ and $[YPYDVPDYA + H]^+$ and that x_n ions are quite rare. Without an arginine residue, the extra proton would be located at one of the peptide bonds or at the *N*-terminus. Regardless, it is unlikely that the attachment of a proton at one of these sites changes the dissociative nature of the excited electronic state(s) accessed at 193 nm in a way that x_n ions are no longer generated.

The most logical explanation for the spectral features presented thus far is that the peptide ions in all the excited electronic states accessed by absorption at 266, 193, or 157 nm undergo rapid internal conversion to the ground electronic state before dissociation. The general trend in the spectral change with the increase in photon energy is that a_n, d_n, x_n, v_n, and w_n ions become gradually more dominant than b_n and y_n ions, which dominate in the low-energy regime, as dictated by the conventional theory. This does not necessarily mean that complete IVR precedes the dissociation step to the extent that all the primary product ions are competitively generated. Dominant cleavages at both ends of an aromatic chromophore observed in 266 nm PD may be

the evidence against the statistical model for PD of peptide ions in the UV range.

It is noted that the repulsive dissociation mechanism is compatible with many of the spectral correlations in PD at 193 and 157 nm, such as the presence of the arginine effect and the absence of the residue-specific effect. In this sense, it may be disappointing that a more comprehensive study suggests dissociations in the ground electronic state. If the primary dissociations of a photoexcited peptide ion occur statistically in the ground electronic state, the characteristics of the PD spectra summarized in the previous section may be explained in terms of the factors affecting the statistical rate constants; namely, the critical energy and the activation entropy. Let us suppose that the acid effect in the low-energy regime arises because of the stabilization of the protonated peptide bond by the adjacent conjugate base of the aspartic or glutamic acid residue and subsequent lowering of the critical energy. As the internal energy substantially increases with the absorption of a 193 nm photon, the influence of the critical energy on the rate constant would become less important than the activation entropy. That is to say, lowering the critical energy through the coordination of the conjugate base at the cost of the activation entropy is not useful in the high-energy regime. Then, the acid effect would not be operative, as seen in the PD spectra.

Even though the proline effect has been known for some time, no detailed studies have been conducted on its mechanistic origin. The implication in previous reports [18, 19] is that this effect may have something to do with the steric effect caused by this cyclic N-alkylated amino acid. Note that cleavage of the bond between the α-carbon and the carbonyl carbon is responsible for most of the major fragment ions observed in 193 nm PD, while the bond cleaved in the low-energy regime is primarily the one between the carbonyl carbon and the amide nitrogen. There is no reason why the steric effect, which is important in the latter case, is also important in the former case. In addition, the increase in the abundance of a_n and x_n ions with the increase in the photon energy suggests that these ions are generated by reaction paths with large entropies of activation. Then, the entropy factor that might have been important in the low-energy regime no longer has a dominant influence on the PD spectral pattern. In this regard, it is interesting to note that a trace of the proline effect might have remained in 193 nm PD of the peptide ions without an arginine residue that mostly generate b_n and y_n ions.

The arginine effect, namely sets of ions (x_n, v_n, w_n) or (a_n, d_n) dominating when an arginine residue is present at the *C*- or *N*-terminus, respectively, is the most striking feature of the 193 and 157 nm PD spectra. In the 266 nm PD spectrum for $[EGVNDNEEGFFSAR + H]^+$ (Figure 7a), x_n ions are weak, even though some v_n and w_n ions are strong. Hence, it cannot be definitely stated that the arginine effect is operative in this case. However, in the 266 nm PD spectrum for $[RLLAPITAY + H]^+$, Figure 7c, a_n and d_n peaks are the major features in the spectrum; x_n ions (x_1 and x_5) appear also, but they are weak. In other words, the position of the arginine residue also seems to affect the appearance of high-energy products, a_n or x_n, in the 266 nm PD, even though the excited electronic state accessed initially is unlikely to be repulsive with respect to the bond between the α-carbon and the carbonyl carbon. However, it is difficult to explain the arginine effect by assuming statistical reactions because hardly any information on the high-energy reaction paths leading to products such as x_n is available. An approximate speculation is as follows. In a singly protonated peptide with arginine at the *C*-terminus, the attached proton is thought to be at the arginine residue. The structure of the x-type ion proposed thus far requires transfer of this proton to the *N*-terminal side of the peptide to generate x_n. In that case, stabilization of the positive charge in x_n by the arginine residue might somehow lead to the preferential formation of x_n. Preferential formation of a_n from the peptide ions with arginine at the *N*-terminus may be similarly explained. However, to proceed beyond the above speculations, detailed studies, such as the quantum chemical search for the reaction paths leading to a_n and x_n, are needed.

Finally, peptides with widely different size, for example RPPGFSPF versus EGVNDNEEGFFSAR, have been investigated in this work. This was to compare with previous results and to develop an overview on the general characteristics of peptide ion dissociation. An interesting observation is that the arginine effect in 193 nm PD seems to operate regardless of the peptide size. This is in apparent contradiction with the statistical argument made to this point. A plausible explanation is that the thermal internal energy of a protonated peptide generated by MALDI also increases with the peptide size and helps to generate high-energy fragment ions in PD. Further studies are needed to establish the photodissociation dynamics for protonated peptides. PD studies on protonated peptides similar in size and with a well-defined internal energy, measurement of photodissociation rate constants, and comparison of the experimental results with statistical rate constants calculated systematically will be useful in this regard.

Conclusions

Photodissociation of various singly protonated peptides was investigated at 193 nm. It was discovered that the proline and the acid effects, which are known to influence the tandem mass-spectral patterns significantly in the low-energy regime, barely operate in 193 nm PD. On the other hand, the presence of an arginine residue and its position inside a peptide was observed to exert a dramatic influence on the overall spectral pattern. The UV-PD spectra obtained at a few wavelengths and the PSD spectra show that the abundance of high-energy fragment ions such as x_n increases as the precursor ion internal energy increases. This suggests that the disso-

ciation of a peptide ion excited by absorption of a UV photon occurs in the ground electronic state, namely after the internal conversion. The influence of the entropy factor, which is known to become increasingly important as the internal energy increases, has been invoked to explain some of the findings such as the absence of the acid effect.

The general trend in UV-PD as mentioned above does not necessarily mean that the dissociation occurs after the quasiequilibrium of the internal energy has been achieved. Since the peptide bonds at both ends of a chromophore preferentially cleave in 266 nm PD, it may evidence against the statistical picture for the dissociation process. In addition, the data presented thus far are insufficient to definitely rule out the possibility that some of the dissociations occur in a dissociative electronic state(s). Further studies are needed to establish the photophysics involved in UV-PD of peptide ions, such as the quantum chemical searches for the reaction paths, and the measurement of the time evolution of product ion signals and their theoretical analysis.

Acknowledgments

This work was supported by CRI, Ministry of Science and Technology, Republic of Korea. The postdoctoral fellowships to JHM and JYO were supported by CRI. SHY thanks the Ministry of Education, Republic of Korea, for the Brain Korea 21 fellowship.

References

1. Busch, K. L.; Glish, G. L.; McLuckey S. A. *Mass spectrometry/Mass spectrometry;* VCH: New York, NY, 1988; pp 107–151.
2. Cole, R. B. *Electrospray ionization mass spectrometry;* Wiley-Interscience: New York, NY, 1997; pp 3–65.
3. Hillenkamp, F; Karas, M; Beavis, R. C; Chait, B. T. Matrix-Assisted Laser Desorption/Ionization Mass Spectrometry of Biopolymers. *Anal. Chem.* **1991,** *63,* 1193A–1202A.
4. Cooks, R. G.; Beynon, J. H; Caprioli, R. M.; Lester, G. R. *Metastable Ions;* Elsevier: Amsterdam, The Netherlands, 1973; pp 89–158
5. Kaufmann, R.; Kirsch, D.; Spengler, B. Sequencing of Peptides in a Time-of-Flight Mass Spectrometer: Evaluation of Postsource Decay Following Matrix-Assisted Laser Desorption Ionization (MALDI). *Int. J. Mass Spectrom. Ion Processes* **1994,** *131,* 355–385.
6. McLafferty, F. W. *Tandem Mass Spectrometry;* Wiley-Interscience: New York, NY, 1983; pp 125–174
7. Cooks, R. G. *Collision Spectroscopy;* Plenum: New York, NY, 1978; pp 357–450
8. Laskin, J.; Furtrell, J. H. Activation of Large Ions in FT-ICR Mass Spectrometry. *Mass Spectrom. Rev.* **2005,** *24,* 135–167.
9. Mabud, M. D. A.; Dekrey M. J.; Cooks, R. G. Surface-Induced Dissociation of Molecular Ions. *Int. J. Mass Spectrom.* **1985,** *67,* 285–294.
10. Laskin, J.; Furtrell, J. H. Collisional Activation of Peptide Ions in FT-ICR Mass Spectrometry. *Mass Spectrom. Rev.* **2003,** *22,* 158–181.
11. Cooper, H. J.; Håkansson, K.; Marshall, A. G. The Role of Electron Capture Dissociation in Biomolecular Analysis. *Mass Spectrom. Rev.* **2005,** *24,* 201–222.
12. Zubarev, R. A.; Horn, D. M.; Fridriksson, E. K.; Keller, N. L.; Kruger, N. A.; Lewis, M. A.; Carpenter, B. K.; McLafferty, F. W. Electron Capture Dissociation for Structural Characterization of Multiply Charged Protein Cations. *Anal. Chem.* **2000,** *72,* 563–573.
13. Bogdanov, B.; Smith, R. D. Proteomics by FTICR Mass Spectrometry: Top Down and Bottom Up. *Mass Spectrom. Rev.* **2005,** *24,* 168–200.
14. Biemann, K.; Martin, S. A. Mass Spectrometric Determination of the Amino Acid Sequence of Peptides and Proteins. *Mass Spectrom. Rev.* **1987,** *6,* 1–75.
15. Robinson, P. J.; Holbrook, K. A. *Unimolecular Reactions;* Wiley-Interscience: New York, NY, 1972; pp 1–108.
16. Forst, W. *Theory of Unimolecular Reactions;* Academic Press: New York, NY, 1793; pp 3–70.
17. Johnson, R. S.; Martin, S. A.; Biemann, K. Novel Fragmentation Process of Peptides by Collision-Induced Decomposition in a Tandem Mass Spectrometer: Differentiation of L and Isoleucine. *Anal. Chem.* **1987,** *59,* 2621–2625.
18. Vaisar, T.; Urban, J. Probing Proline Effect in CID of Protonated Peptides. *J. Mass Spectrom.* **1996,** *31,* 1185–1187.
19. Breci, L.; Tabb, D. L.; Yates, J. R.; Wysocki, V. H. Cleavage, N-Terminal to Proline: Analysis of Database of Peptide Tandem Mass Spectra. *Anal. Chem.* **2003,** *75,* 1963–1971.
20. Wysocki, V. H.; Tsaprailis, G.; Smith, L. L.; Breci, L. A. Mobile and Localized Protons: A Framework for Understanding Peptide Dissociation. *J. Mass Spectrom.* **2000,** *35,* 1399–1406.
21. Park, S. T.; Kim, S. K.; Kim, M. S. Observation of Conformation-Specific Pathways in the Photodissociation of 1-Iodopropane Ions. *Nature* **2002,** *415,* 306–308.
22. Park, S. T.; Kim, M. S. Photodissociation Dynamics of Various Conformers of Iodobutane Isomer Ions Prepared Selectively by Vacuum Ultraviolet Mass-Analyzed Threshold Ionization. *J. Am. Chem. Soc.* **2002,** *124,* 7614–7621.
23. Oh, J. Y.; Moon, J. H.; Kim, M. S. Tandem Time-of-Flight Mass Spectrometer for Photodissociation of Biopolymer Ions Generated by Matrix-Assisted Laser Desorption Ionization (MALDI-TOF-PD-TOF) Using a Linear-Plus-Quadratic Potential Reflectron. *J. Am. Soc. Mass Spectrom.* **2004,** *15,* 1248–1259.
24. Moon, J. H.; Yoon, S. H.; Kim, M. S. Construction of an Improved Tandem Time-of-Flight Mass Spectrometer for Photodissociation of Ions Generated by Matrix-Assisted Laser Desorption Ionization (MALDI). *Bull. Korean Chem. Soc.* **2005,** *26,* 763–768.
25. Moon, J. H.; Yoon, S. H.; Kim, M. S. Enhancement of Matrix-Assisted Laser Desorption/Ionization Photodissociation Tandem Time-of-Flight Mass Spectra; Spectral Reduction and Cleanup of Isotopomeric Contamination. *Rapid Commun. Mass Spectrom.* **2005,** *19,* 2481–2487.
26. Cui, W.; Thomson, M. S.; Reilly, J. P. Pathways of Peptide Ion Fragmentation Induced by Vacuum Ultraviolet Light. *J. Am. Soc. Mass Spectrom.* **2005,** *16,* 1384–1398.
27. Barbacci, D. C.; Russell, D. H. Sequence and Side-Chain Specific Photofragment (193 nm) Ions from Protonated Substance P by Matrix-Assisted Laser Desorption Ionization Time-of-Flight Mass Spectrometry. *J. Am. Soc. Mass Spectrom.* **1999,** *10,* 1038–1040.
28. Moon, J. H., Yoon, S. H., Kim, M. S. A Deflection System to Reduce the Interference from Post-Source Decay Product Ions in Photodissociation Tandem Time-of-Flight Mass Spectrometry. *Rapid Commun. Mass Spectrom.* in press.
29. Rosenstock, H. M.; Wallenstein, M. B.; Wahrhaftig, A. L.; Eyring, H. Absolute Rate Theory for Isolated Systems and the Mass Spectra of Polyatomic Molecules. *Proc. Nat. Acad. Sci. U.S.A.* **1952,** *38,* 667–678.
30. Oh, J. Y.; Moon, J. H.; Kim, M. S. Sequence- and Site-Specific Photodissociation at 266 nm of Protonated Synthetic Polypeptides Containing a Tryptophanyl Residue. *Rapid Commun. Mass Spectrom.* **2004,** *18,* 2706–2712.
31. Oh, J. Y.; Moon, J. H.; Kim, M. S. Chromophore Effect in Photodissociation at 266 nm of Protonated Peptides Generated by Matrix-Assisted Laser Desorption Ionization (MALDI). *J. Mass Spectrom.* **2005,** *40,* 899–907.
32. Martin, S. A.; Hill, J. A.; Kittrell, C.; Biemann, K. Photo-Induced Dissociation with a Four-Sector Tandem Mass Spectrometer. *J. Am. Soc. Mass Spectrom.* **1990,** *1,* 107–109.
33. Williams, E. R.; Furlong, J. J. P.; McLafferty, F. W. Efficiency of Collisionally-Activated Dissociation and 193 nm Photodissociation of Peptide Ions in Fourier Transform Mass Spectrometry. *J. Am. Soc. Mass Spectrom.* **1990,** *1,* 288–294.
34. Robin, M. B. *Higher Excited States of Polyatomic Molecules,* Vol. II; Academic Press: New York, NY, 1974; pp 122–155.
35. Morgan, J. W.; Russell, D. H. Comparative Studies of 193 nm Photodissociation and TOF-TOFMS Analysis of Bradykinin Analogs: The Effects of Charge Site(s) and Fragmentation Timescales. *J. Am. Soc. Mass Spectrom.* **2006,** *17,* 721–729.
36. Thomson, M. S.; Cui, W.; Reilly, J. P. Fragmentation of Singly Charged Peptide Ions by Photodissociation at $\lambda = 157$ nm. *Angew. Chem. Int. Ed.* **2004,** *43,* 4791–4794.
37. Moon, J. H.; Yoon, S. H.; Kim, M. S. Photodissociation of Singly Protonated Peptides at 193 nm Investigated with Tandem Time-of-Flight Mass Spectrometry. *Rapid Commun. Mass Spectrom.* **2005,** *19,* 3248–3252.